Metastable Ferrous Austenite - Consequences on Fracture and Tribology

I. Schmidt, Zahnradfabrik Friedrichshafen AG, Friedrichshafen, FRG

Introduction

It is well known that a certain number of austenitic or partially austenitic alloys exhibit drastical changes of properties when these materials can undergo a martensitic transformation induced by deformation. These changes can refer to e.g. density, shape, hardness, strength, ductility, fatigue crack growth, fracture toughness, wear resistance, corrosion resistance, permeability.

It is the aim of the present paper to explain the principle mechanism and to demonstrate the necessary prerequisites which must be fulfilled if metastable ferrous austenites should be turned to a good account in mechanical engineering. Aspects on fracture and wear resistance are placed into the foreground.

General Aspects

Since the work of Scheil (1) in 1932 concerning the effects of stress on the formation of martensite many investigations have been made in this field. Among the phenomena that have been observed are the change in the martensite start temperature M_s with the application of stress, the stimulation of martensite formation by plastic deformation, mechanical stabilization effects. The main aspects have been summarized and discussed in general (review) articles on the martensitic transformation (2 - 7). A systematic analysis of the effect of all variables on the martensitic transformation temperatures is given by Hornbogen (8). The following concentrates on essentials.

Stable austenites never transform to martensite. They are found in tough structural alloy steel, high alloy stainless steel or casting, wear resistant steel. The latter is known as Hadfield steel (Fe-12Mn-1.2C). Its high work-hardening rate is explained by the large composition of substitutional atoms (Mn) which considerably lowers the stacking fault energy and by dynamic strain aging brought about by the reorientation of carbon atoms or carbon -manganese couples in the cores of dislocations (9).

In metastable austenites an additional contribution to rapid work-hardening is due to the deformation-induced generation of martensite. The martensitic transformation starts spontaneously on cooling at $M_s = T_o - \Delta T$. Above M_s it can be induced by external stresses. This stress-induced phase transformation occurs when a shear stress τ_{aM} acts in the direction of the martensitic shear which would have occured below M_s without the application of external forces. τ_{aM} is zero at the martensite start temperature M_s, and increases with decreasing undercooling $\Delta T < T_o - M_s$, i.e. with decreasing chemical driving force for the martensitic transformation (Fig.1 (10, 7). It has been observed (11) that at tem-

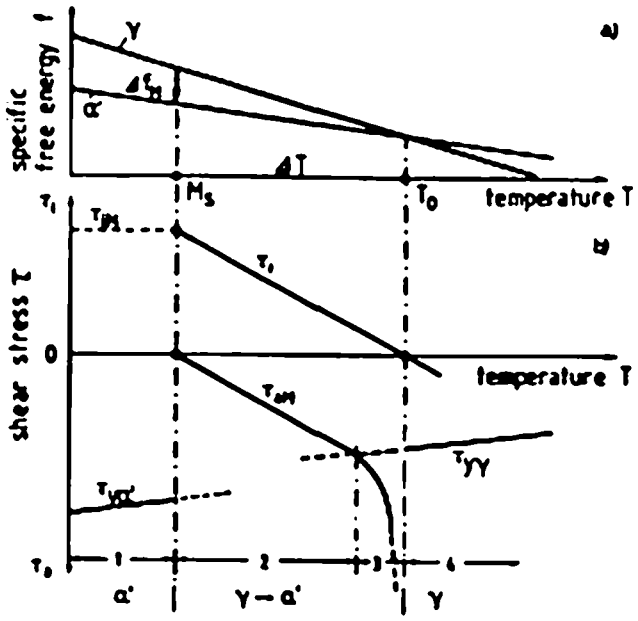

Fig. 1: Schematic representation of thermo-dynamical and mechanical properties of an undercooled high temperature phase γ (10). a) Temperature dependence of specific free energy f of the phases γ and α' b) At $T < T_0$ the internal shear stress increases which induces spontaneous transformation at $\tau_i = \tau_{iM}$. According to the undercooling ΔT the external shear stress τ_{aM} necessary to cause transformation is reduced due to an increasing internal shear stress τ_i. τ_{aM} becomes zero at $T = M_s$.

Range 1: γ/α'-transformation occurs by cooling. External shear stress is not necessary.
Range 2: γ/α'-transformation induced by stress.
Range 3: Deformed austenite, strain-induced martensitic transformation.
Range 4: Stable austenite, work-hardening due to defects, no martensite is formed.

peratures near M_s the transformation mode is dominated by stress-assisted nucleation on the same sites responsible for the spontaneous cooling transformation. In a higher temperature regime, however, strain-induced nucleation of martensite on new sites produced by plastic deformation (eg. slip bands, - crossings) is found. Above the M_d-temperature a deformation-induced martensitic transformation is impossible. It is worth mentioning that the equilibrium temperature T_0 depends on the chemical composition of alloy, the degree of order, the hydrostatic stress; the necessary undercooling ΔT is influenced by the nucleation and growth conditions for martensite inside the matrix which depend on the external shear stress and strength of austenite (8). The quantitative connection between the change of M_s and the external shear stress τ_a with its component τ_{aM} parallel to the martensitic shear ϕ_M is given by equ.1 (3, 10, 12).

$$\frac{dM_s}{d\tau_{aM}} = \frac{\Phi_M}{\Delta s_M} \qquad \text{Equ. 1}$$

Due to the different transformation entropies Δs_{η} this effect is small in steels (Fig. 2 (2)), but large in Cu- or NiTi-base shape memory alloys (12, 13).

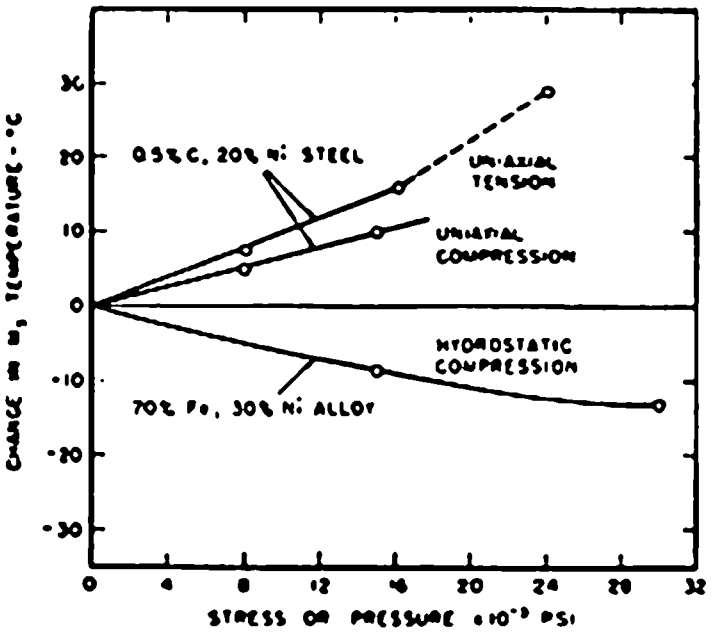

Fig. 2: Change in M_s temperature as a function of loading condition (2)

Fracture of Metastable Austenite

The unusual combination of strength, ductility and toughness exhibited by metastable austenites have called much attention to the potential benefits of deformation-induced martensitic transformation. Consequences such as high fracture toughness, increased fatigue life and TRansformation Induced Plasticity (TRIP) are discussed in the following.

Fracture Toughness and Fatigue Strength

It has been shown for e.g. metastable austenitic stainless steels (Fe-16Cr-13Ni, Fe -18Cr-6.5Ni-0.19C (14)), Fe-29Ni-7Al alloys (15, 16), austempered ductile irons with high amounts of retained metastable austenite (17) that a local strain-induced $\gamma - \alpha'$ transformation at the crack tip takes place (Fig. 3 (15)). This leads to a compressive internal stress state ($\Delta V_{\gamma\alpha'}/V_{\gamma} > 0$) which relieves the crack tip and impedes crack propagation. As compared to the deep-cooled fully martensitic microstructure (and stable austenite of slightly modified chemical composition) drastical decreases of the fatigue crack growth rates are observed. Fig. 4a exemplifies the situation of an Fe-29Ni-7Al alloy; in addition, it reveals the high fracture toughness which even increases with specimen thickness, and the relatively high threshold value for fatigue crack growth of transformable austenites (15). It must be mentioned, however, that the optimum effect is strongly temperature dependent. For a given stress intensity the amount of strain-induced martensite in the plastic zone decreases and the crack propagation rate increases with increasing temperature. This is shown in Fig. 4b (14).

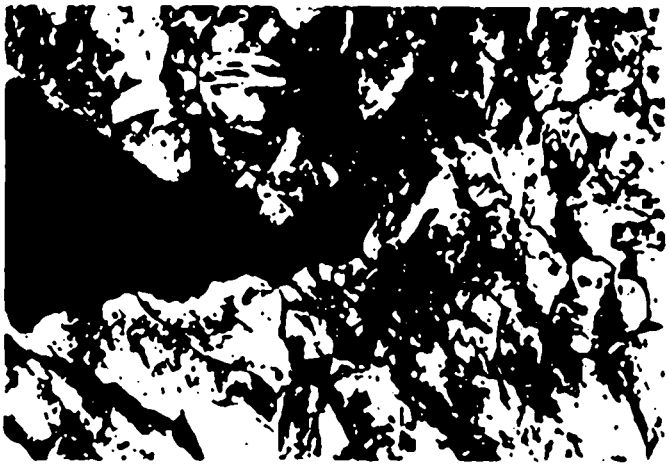

Fig. 3: Metallographic investigation of the transformation at the crack tip (15)

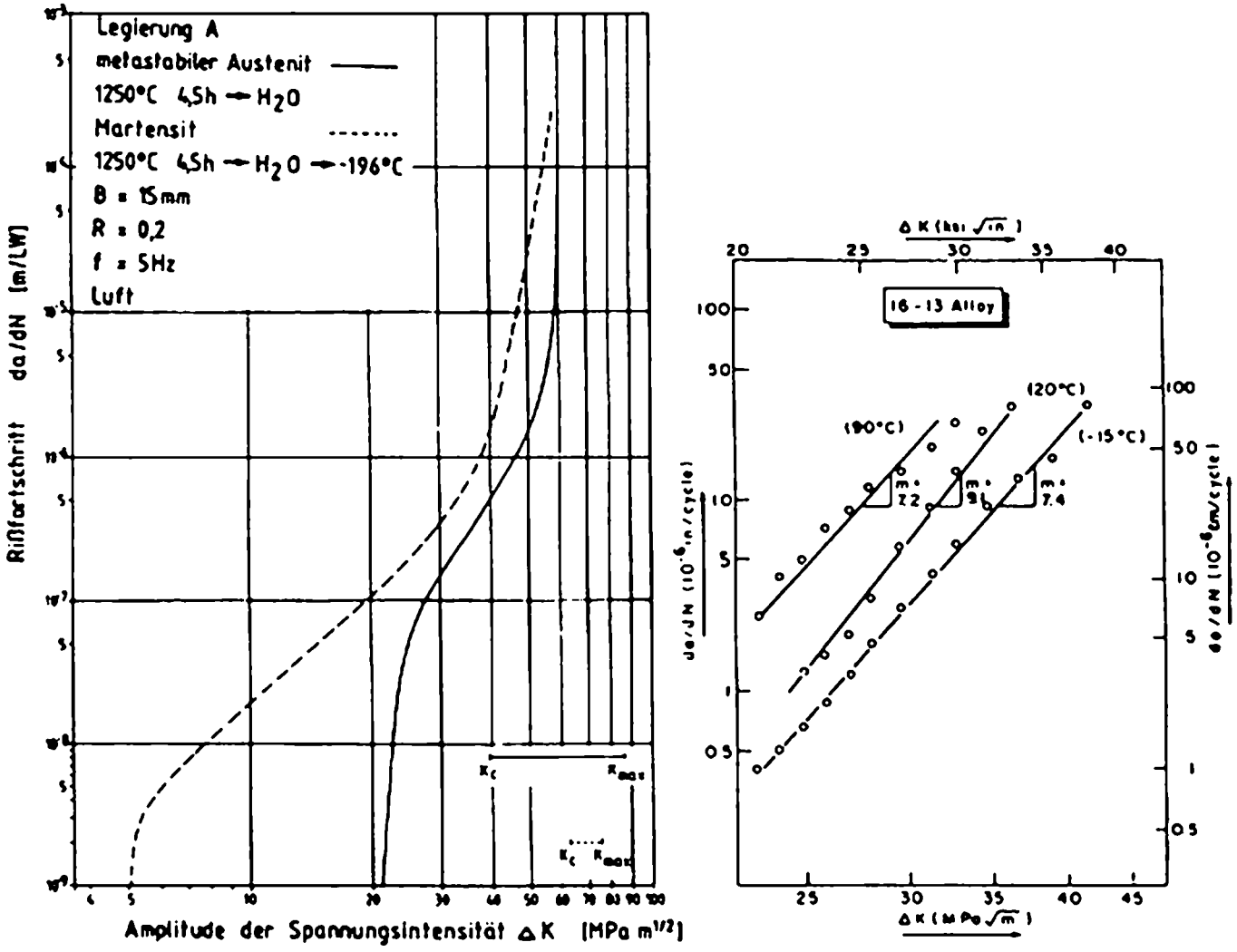

Fig. 4: Fatigue crack growth rates da/dN = f(ΔK) for cyclic tension. a) Comparison of martensitic and austenitic structure (Fe-29Ni-7Al (17)), b) influence of test temperature (Fe-16Cr-13Ni, M_s = -75 °C, M_d = +80 °C (14))

The influence of deformation-induced martensitic transformation on the fatigue properties of metastable austenitic steels is strongly dependent on the respective test conditions. Stress-controlled fatigue tests show that martensitic transformation is beneficial to the fatigue life; on the contrary, the martensitic transformation shortens the fatigue life in the strain-controlled tests (18). In addition, it has been reported that the influence of deformation-induced martensitic transformation on the fatigue life is closely related to the threshold number of cycles for the onset of martensite formation. However, up to now, critical conditions for the onset as well as kinetics of the deformation-induced phase transformation during fatigue are not well understood as compared to those during monotonic tensile or compressive deformation (19).

Transformation Induced Plasticity

Fig. 5 shows the stress-strain curves of the Fe-29Ni-0.26C austenitic alloy (M_s = -60 "C, M_d = +25 "C) deformed in tension at various temperatures (20). At -50 "C and at -70 "C, i.e. near the M_s temperature, large serrations due to the stress-induced martensitic transformation are observed before yielding of austenite. At elevated temperatures (-10 "C or -30 "C) fine serrations indicate that martensite is formed gradually with strain after yielding of austenite. Consequently a large elongation is observed which in the case of an Fe-25Ni-0.37C alloy can surpass 200 % (21).

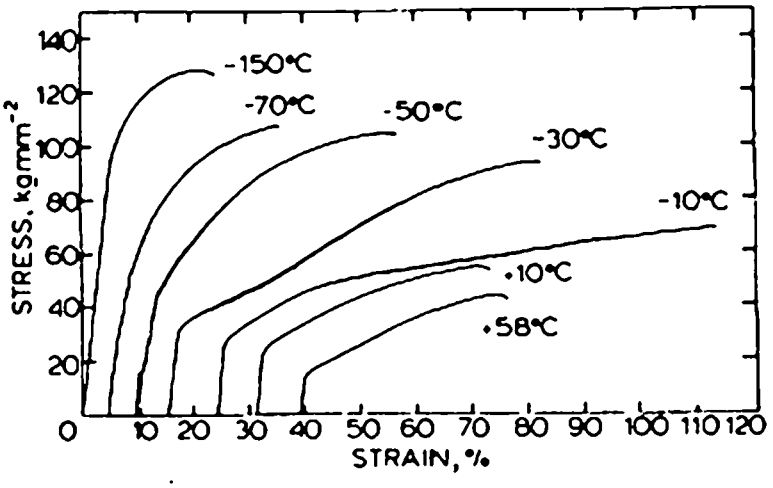

Fig. 5: Stress-strain curves of Fe-29Ni-0.29C alloy (M_s = -60 "C, M_d = +25 "C) during tensile tests at various temperatures, $\dot{\varepsilon} = 5.5 \times 10^{-4}\ s^{-1}$ (20)

The tensile strength decreases with increasing test temperature, which corresponds to the decreasing volume fraction of martensite measured in the specimen after fracture. The total elongation exhibits a maximum at -10 "C. It is assumed that this temperature is just above M_s^{σ}, when the transformation mode changes from a stress-assisted to a strain-induced one. Such an enhancement of elongation is mainly attributed to the suppression of necking (i.e. the enhancement of uniform elongation) due to the continuous increase of work-hardening rate by the martensitic transformation. In addition, this behaviour effects a retardation of the initia-

tion and the propagation of cracks because the stress concentrations may be relaxed by the formation of preferential martensite variants in stress-concentrated regions.

Application to Practical Engineering

As mentioned above, the elongation and ductility can be enormously enhanced by TRIP, but the increase in yield strength has to be achieved by other means. Two-phase alloys of ausformed martensite (strength) and retained metastable austenite (TRIP) are the consequent development (6). In addition, ausaging, maraging, strain aging can also improve the strength of TRIP steels. The result is the combination of tensile strength in the range of 2.000 MPa and elongation above 25 %, Tab. 1 (6).

These properties combined with good corrosion resistance fulfil the requirements for pressure vessels, structural materials, chemical plants, off-shore developments, armour-plates, dampers. However, some undesirable consequences, most notably inhomogeneous yielding and extreme temperature sensitivity have hampered the practical development and application of the high-strength TRIP steels (22, 23). In the optimum temperature range only a small amount of adiabatic heating is required to drastically alter the shape of stress-strain curve with an attendant serious loss of uniform ductility.

C	Si	Mn	Cr	Mo	NI	Fe
0.3	2	2	9	4	8	balance
0.2	2	2	13	3	9	balance
0.25	2	1	13	3	8	balance

Tab. 1: Typical high strength TRIP steel compositions (w/o)

For increasing fatigue strength (rotating or alternating bending) of structural components case-hardening of steels plays the most important role in practical application. Optimization efforts are always attended with e.g. the case-hardening depth, hardness profile, bulk and superficial C-content and retained austenite in the carburized layer. The origin and effects of retained austenite in these steels are comprehensively summarized by Razim (24) according to which maximum fatigue life is found for the minimum amount of retained austenite. It is the consequence of the maximum amount of residual compressive stresses obtained by case-hardening. The stress-induced martensitic transformation of retained austenite in case-carburized steels is also described and a positive effect on fatigue strength is reported in comparison with deep-frozen martensitic structures (25, 26).

Tribological Properties of Metastable Austenite

Basically, the martensitic transformation in frictioned surfaces of ferrous alloys is caused by two different effects. On the one hand, in ferritic steels (M_s > ambient temperature) a friction-

induced temperature pulse can lead to austenitization and subsequent martensitic transformation. This martensite is deformed by frictional forces and the "white martensite" is formed. Its inner structure is characterized by a very high density of dislocations to which carbon atoms have segregated (27, 28).

In metastable austenitic steels exposed to friction below M_d surface martensite is caused by the friction-induced shear stress (29). This external shear stress is exerted parallel to the surface. It is proportional to the coefficient of friction μ of the respective frictional system and the amount of the compressive stress $|-\sigma|$:

$$|-\sigma| \cdot \mu = \tau_e \qquad \text{Equ. 2}$$

Superimposition of compressive stress and frictional shear stress creates a triaxial stress state. This external stress field gives a variable shear stress component to the active shear system of the martensite depending on its orientation. If this component surpasses a critical value $\tau_{\alpha M}$ martensite nuclei form (Fig. 1). Therewith, the transformed volume, i. e. the thickness of the friction-induced martensitic layer is a function of the strength of austenite, its thermo-dynamic stability and the extent of the external stress field. Referring to wear the advantage of this phenomenon is that maximum strengthening is produced at the particular site which is exposed to the highest frictional loads and that renewable hard surface layers are created.

Austenitic Manganese Steels

The classic Hadfield steel (Fe-12Mn-1.2C) exhibits a marked wear resistance to heavy impact and gouging abrasion. It is not especially resistant to low stress abrasion (30, 31), because of the lack of hard dipersions or martensite. Systematic decreasing of austenite stability by decreasing the Mn- and/or C-content involves the formation of friction-induced martensite (Fig. 6). It leads to a continuous increase of surface hardness as well as of wear resistance (32). The plot of Fig. 6 confirms that the particular wear resistance cannot be related to the bulk hardness H_o of the virgin austenite, but to the surface hardness $H_o + \Delta H$ resulting from work-hardening during sliding (29):

$$W^1 \sim H_o + \Delta H \qquad \text{Equ. 3}$$

At relatively low frictional loads the linear relationship indicates that the continuous transition from pure work-hardening of austenite (12Mn, 8Mn) to friction-induced martensitic transformation in a thin frictioned layer (5 Mn) does not change the wear mechanism. Microcutting and microploughing predominate. If, however, the transformed layer exceeds a certain thickness, a brittle fracture component arises and the wear resistance decreases independently of the maximum surface hardness (Fig. 7).

Differences in wear mechanisms are described by the coefficient of wear k which expresses the probability of decohesion of matter in the asperity area A (34). (A_o is the nominal surface of the sliding material.) It has been proposed to subdivide the coefficient of wear k into two components characterizing deformation (k_d) and brittle fracture (k_f) (35, 36):

$$W = k \cdot \frac{A}{A_o} = k \cdot \frac{\sigma}{H_o + \Delta H} = (k_d + k_f) \cdot \frac{\sigma}{H_o + \Delta H} \qquad \text{Equ. 4}$$

Alloy No.	Chemical comp., w/o Mn	C	Si	M_s/°C	$\overline{HV10}_{RT}$	$\overline{HV10}_{-32}$
12 Mn	13.4	1.14	0.43	<<-196	223.3	223.3
8 Mn	7.75	1.16	0.33	< -196	224.3	224.3
6 Mn	6.03	1.16	0.29	- -196	223.8	228.8
5 Mn	4.98	1.16	0.31	- 57	219.3	368.5
4 Mn	3.97	1.15	0.29	- 31	218.1	436.0
8 Mn0.7C	8.30	0.69	0.22	- 2	228.2	524.3

0.03 P, < 0.01 S, < 0.04 Al

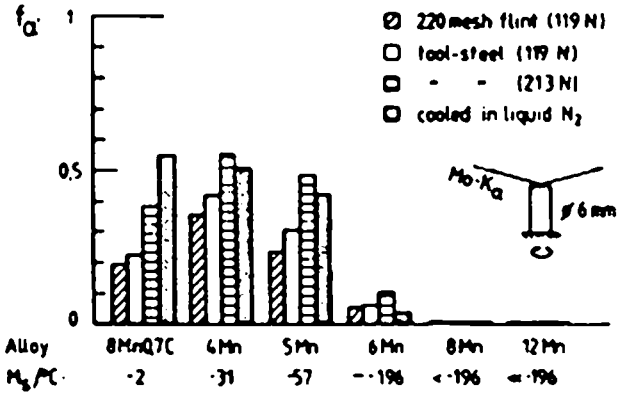

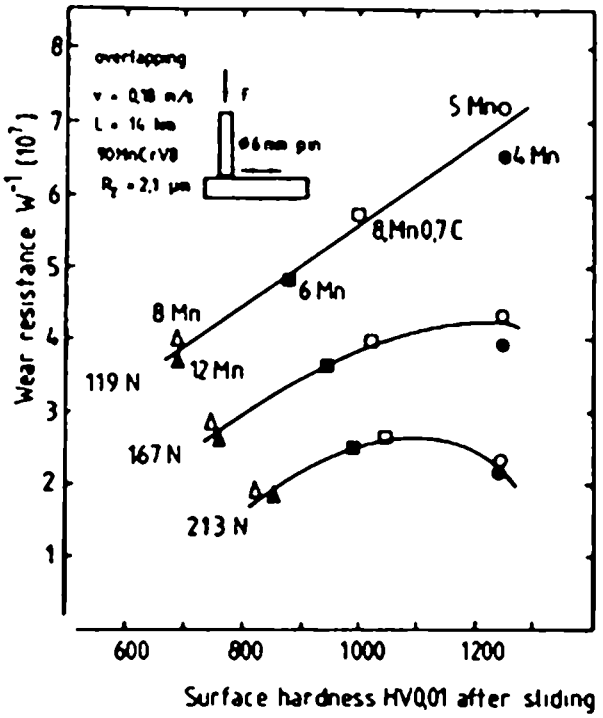

Fig. 6: a) alloys investigated b) plot of martensitic volume fraction $f_{\alpha'}$ due to friction or cooling in liquid N_2 vs. the degree of metastabilitiy of austenite. c) influence of the applied load on wear resistance and surface hardness after dry sliding

Fig. 7: Brittle fracture in a martensitically transformed surface layer of the alloy 4Mn exposed to dry sliding, M_s = -31 °C, tool-steel counterpart, app. pressure p* = 38.2 MPa (32) a) LM, b) SEM

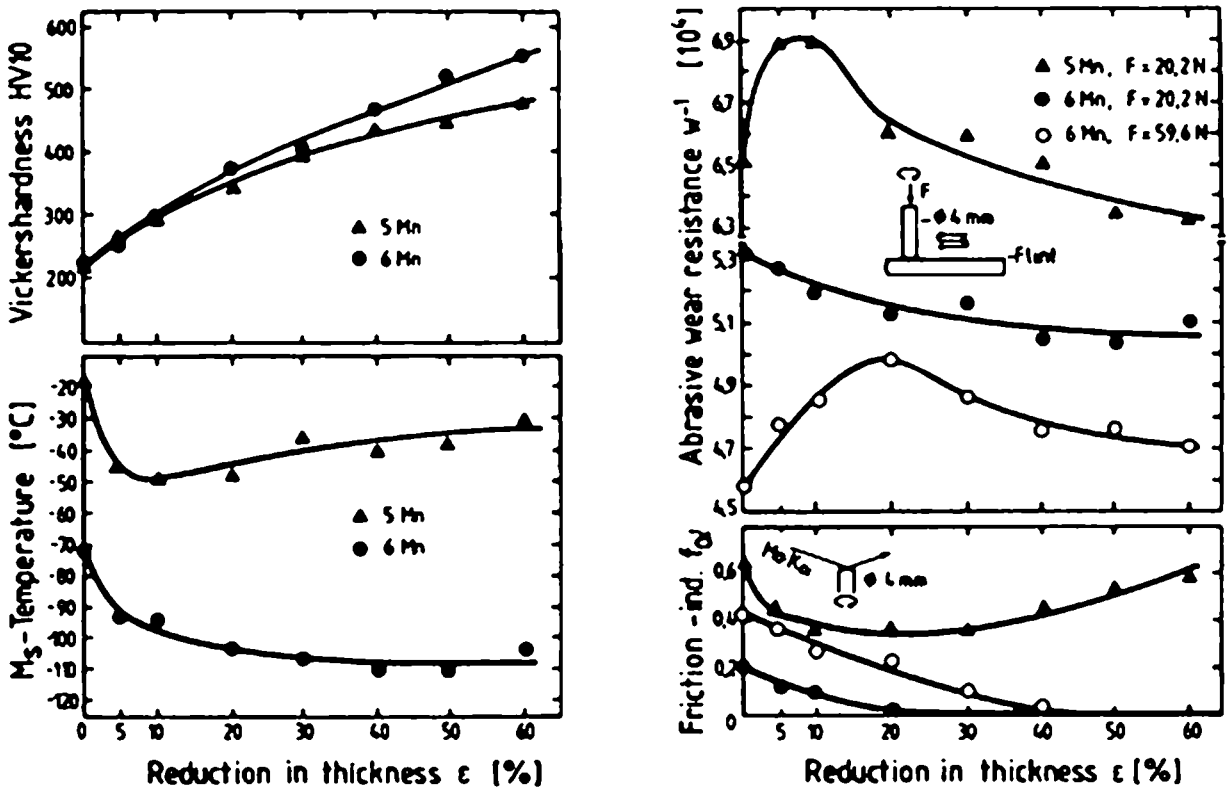

Fig. 8: a) Influence rolling of above M_d on Vickers hardness and M_S, b) plot of abrasive wear resistance and amount of friction-induced martensite vs. deformation of austenite above M_d

It seems to be reasonable from the results presented that in less stable high-carbon austenitic alloys this brittle fracture component controls the wear rate. It is most effective in thick martensitic layers as unstable crack growth cannot be prevented. Obviously, in these alloys the change in hardness due to the friction-induced martensitic transformation is overcompensated by a decrease in fracture energy of the transformed layer (36). This is most pronounced during wear of metastable austenites at high loads.

Predeformation of these austenites e.g. by rooling above the M_d temperature (M_d > 400 °C) which influences the M_s temperature by work-hardening $d\sigma/d\varepsilon$, internal stresses $d\tau_i/d\varepsilon$, and new possible nucleation sites for martensite $dn_N/d\varepsilon$ at slip bands or slip band crossings (37, 38) seems to be a suitable preconditioning process for better accommodation of austenite to the conditions of the respective wear system (39) (Fig. 8):

$$\frac{dM_s}{d\varepsilon} = -\frac{\partial \Delta T}{\partial \tau_y} \cdot \frac{\partial \tau_y}{\partial \varepsilon} + \frac{\partial \Delta T}{\partial \tau_i} \cdot \frac{\partial \tau_i}{\partial \varepsilon} + \frac{\partial \Delta T}{\partial n_N} \cdot \frac{\partial n_N}{\partial \varepsilon} \qquad \text{Equ. 5}$$

Retained Austenite in Alloys Approved in Service

The results obtained in austenitic model alloys mentioned above can easily be related to multi-phase alloys in practical engineering consisting of more or less amounts of retained austenite.

Ledeburitic high-alloy Fe-Cr-C tool-steels consist of a fine dispersion of M_7C_3 -carbides embedded in a hardened, mainly martensitic matrix. It has been shown that an increasing amount of retained austenite leads to a significant decrease in wear rate (Fig. 9, X210Cr12 + 12 v/o TiC) (40).

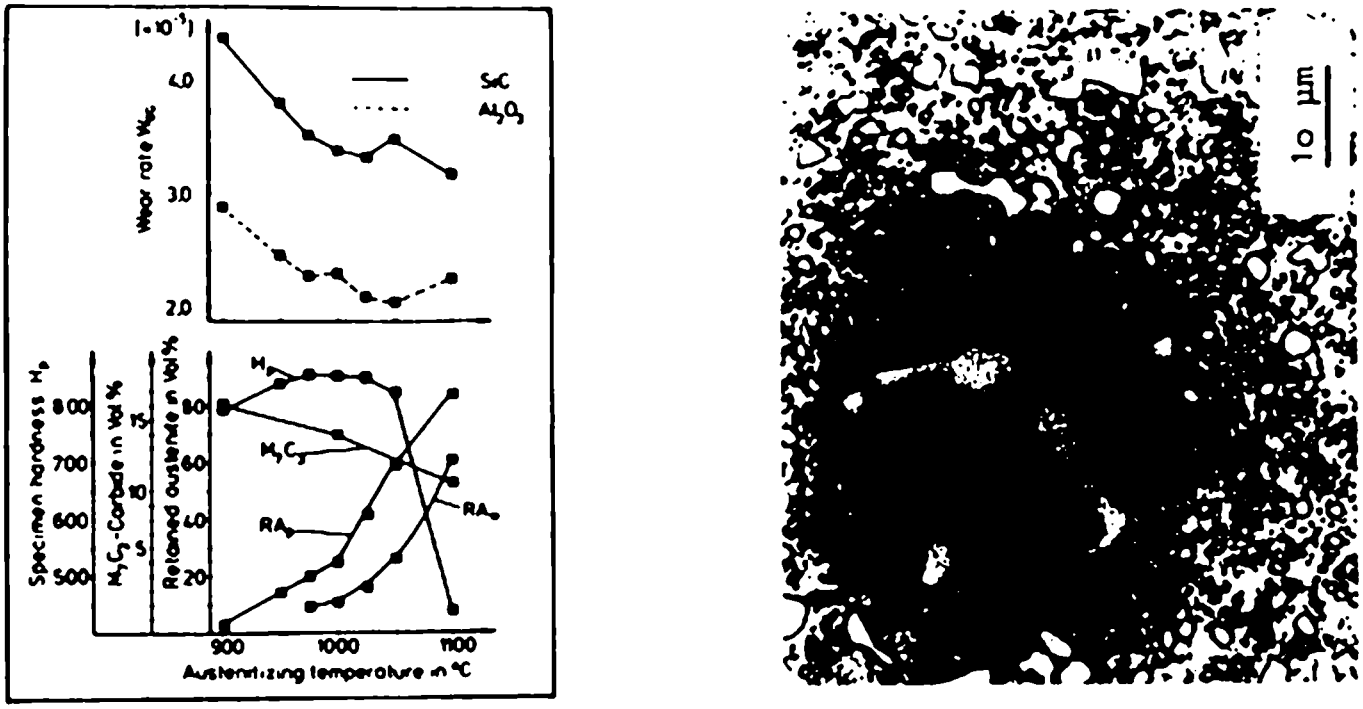

Fig. 9: a) abrasive wear rate in dependence of macrohardness, amount of carbides and retained austenite before (RA_ρ) and after (RA_w) sliding on SiC and Al_2O_3 b) LM of X210Cr12, 30'/900"C/oil

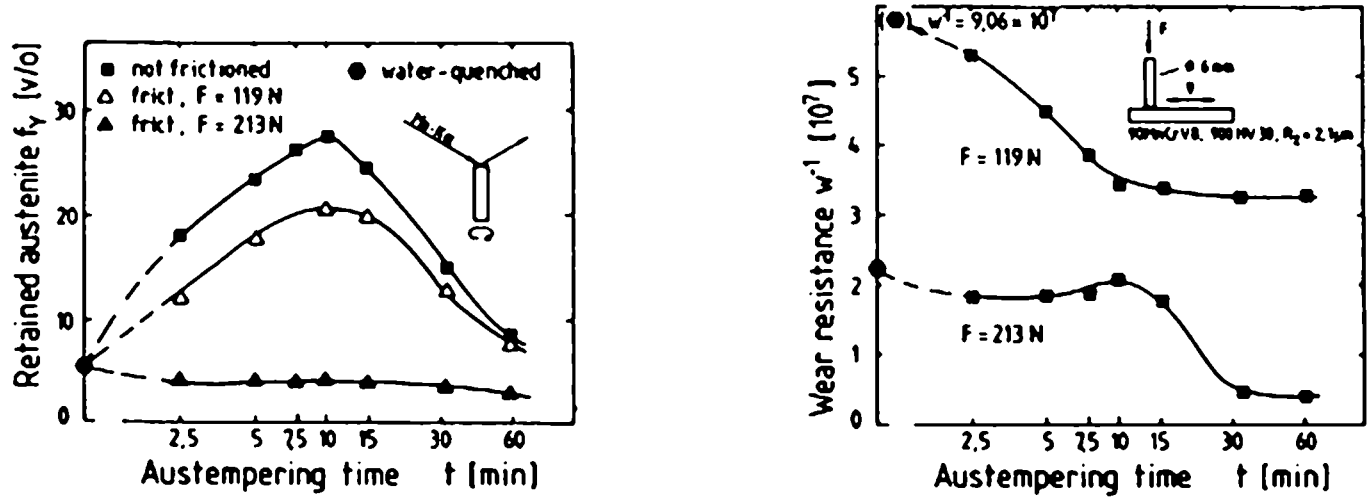

Fig. 10: Connection between the amount of retained austenite before and after friction and the sliding wear resistance as a function of austempering time (T = 400 "C).

Austempered ductile irons (e.g. GGG 100BA) combine excellent mechanical properties such as tensile strengths between 800 and 1600 MPa, elongations at fracture ranging from 16 to 1%, fatigue limits comparable to those of tempered wrought steels with very high wear resistance under abrasive conditions (41, 42, 43). These characteristics originate from the special micostructure. It consists of about 12 v/o carbon sperulites and a fine-scaled mixture of bainite and austenite which is obtained by austenitization and subsequent austempering in the bainite range. Depending on the applied frictional shear stress, the amount of retained austenite and its thermo-dynamic stability the wear resistance of a tough austempered ductile iron can approach values of quench-hardened ductile iron (Fig. 10 (42)).

In roller bearing steels (e.g. 100Cr6, Fig. 11 (44)) as well as in gear wheel steels (e.g. 16MnCr5, 15CrNi6) transformation of retained austenite due to the Hertzian contact stress field during service has been observed. However, no worth mentioning influence on dimensional stability or performance is found if the correct heat treatment is conducted before.

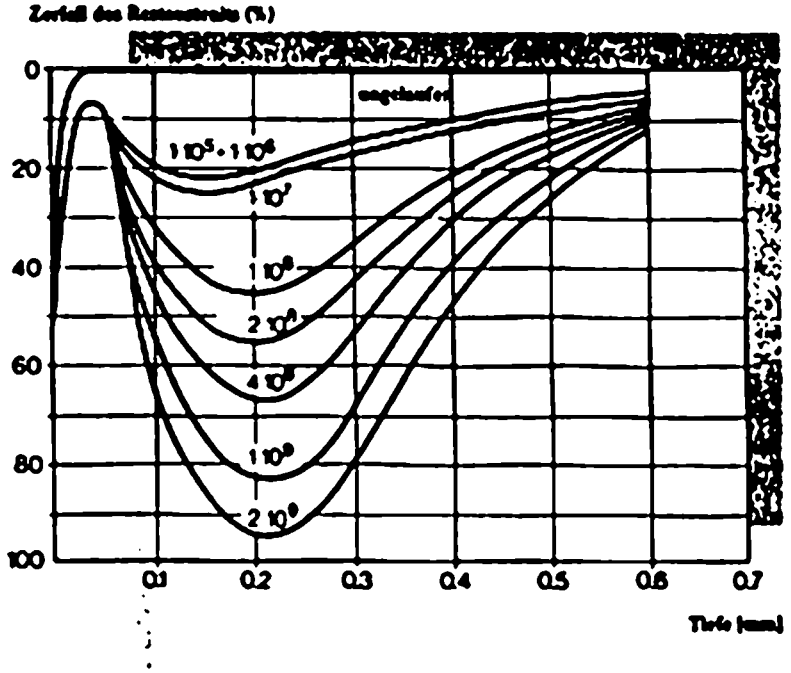

Fig. 11: Transformation of the retained austenite in 100Cr6 in dependence of the depth below the roller path and revolutions, contact stress σ_H = 3800 MPa (44)

References

(1) E. Scheil: Z. Anorg. Chem. 207 (1932) 21
(2) J. R. Patel, M. Cohen: Acta metall. 1 (1953) 531-538
(3) U. Dehlinger: Theoretische Metallkunde, 1. Edition, Springer, Berlin, 1955, p. 168
(4) L. Kaufman, M. Cohen: Prog. Met. Phys. 7 (1958) 165-246

(5) E. Hornbogen, G. Wassermann: Z. Metallkde. 47 (1958) 427-433
(6) V. F. Zackey, E. R. Parker, D. Fahr, R. Busch: Trans. ASM 60 (1967) 252-259
(7) I. Tamura: Metal Science 16 (1982) 245-253
(8) E. Hornbogen: Acta metall. 33 (1985) 595-601
(9) Y. N. Dastur, W. C. Leslie: Met. Trans. 12A (1981) 749-759
(10) E. Hornbogen: Z. Metallkde. 75 (1984) 739-746
(11) G. B. Olson, M. Cohen: J. Less-Common Met. 28 (1972) 107-118
(12) E. Hornbogen: Arch. Eisenhüttenwes. 43 (1972) 307-313
(13) H. Warlimont, L. Delaey, R. V. Krishnan, H. Tas: J. Mater. Sci. 9 (1974) 1545-1555
(14) A. G. Pineau, R. M. Pelloux: Met. Trans. 5 (1974) 1103-1112
(15) I. Wittkamp, E. Hornbogen: Prakt. Metallographie 14 (1977) 237-250
(16) E. Hornbogen: Acta metall. 26 (1978) 147-152
(17) K. H. Bowe, E. Hornbogen, M. Hühner: konstr. + gießen 12 (1987) 14-19
(18) G. B. Olson, R. Chait, M. Azrin, R. G. Gagne: Met. Trans. 11A (1980) 1069-1080
(19) K. Tzusaki, T. Maki, I. Tamura: J. Phys. 12 (1982) 423-428
(20) I. Tamura, T. Maki, H. Hato: Trans. Iron Steel Inst. Japn, 10 (1970) 163-171
(21) I. Tamura, Y. Tomota, M. Ozawa: The microstructure and design of alloys, The Metals Society, London, 1974, p. 540
(22) M. Azrin, G. B. Olson, R. A. Gagne: Mat. Sci. Eng. 23 (1976) 33-41
(23) G. B. Olson, M. Cohen: Met. Trans. 13A (1982) 1907-1914
(24) C. Razim: HTM 40 (1985) 150-165
(25) H. Brandis, H. Reimers, W. Schmidt, A. Von den Steinen: ibid. 38 (1983) 63-70
(26) H. Brandis, H. Dietrich, W. Schmidt: ibid. 40 (1985) 57-63
(27) H. Uetz, K. Sommer: Mineralöltechnik 12 (1972) 3-25
(28) E. Minuth, E. Hornbogen: Prakt. Metallogr. 13 (1976) 584-598
(29) H.-M. Bauschke, K.-H. Zum Gahr, E. Hornbogen: Z. Metallkde. 72 (1981) 1-12
(30) H. Berns, H. F. Klärner, E. Schmidtmann: Arch. Eisenhüttenwes. 38 (1967) 447-453
(31) D. E. Diesburg, P. Borik: Symp. Materials for the Mining Industry, Climax Molybdenum Company, Vail, CO, (1974) 15-41
(32) N. Jost, I. Schmidt: Wear 111 (1986) 377-389
(33) I. Schmidt: Z. Metallkde. 75 (1984) 747-754
(34) J. P. Archard: J. Appl. Phys. 24 (1953) 981-988
(35) E. Hornbogen: Z. Metallkde. 66 (1975) 507-510
(36) K.-H. Zum Gahr: ibid. 69 (1978) 643-650
(37) H. Onodera, I. Tamura: J. Phys. 12 (1982) 337-342
(38) R. D. Wollmann, J. R. C. Guimaraes: Scripta Met. 7 (1973) 355-360
(39) I. Schmidt, M. Wilhelm: ibid. 78 (1987) 127-130
(40) H. Berns, W. Trojahm: Z. Werkstofftechn. 14 (1983) 382-389
(41) P. Mayr, H. Vetters, J. Walla: Gießereiforschung 38 (1986) 86-92
(42) I. Schmidt, A. Schuchert: Z. Metallkde. 78 (1987) 871-875
(43) S. Shepperson, C. Allen: Proc. Int. Conf. on Wear of Materials, ASME, K. C. Ludema (ed.), Houston TX (1987) 573-583
(44) G. E. Hollux, A. P. Voskamp, E. Ionnides: Kugellager-Zeitschrift 231 (1989) 20-27